# Multidecadal Mobility of the North Atlantic Oscillation

G. W. K. MOORE

*Department of Physics, University of Toronto, Toronto, Ontario, Canada*

I. A. RENFREW

*School of Environmental Sciences, University of East Anglia, Norwich, United Kingdom*

R. S. PICKART

*Department of Physical Oceanography, Woods Hole Oceanographic Institution, Woods Hole, Massachusetts*

(Manuscript received 29 December 2011, in final form 3 June 2012)

ABSTRACT

The North Atlantic Oscillation (NAO) is one of the most important modes of variability in the global climate system and is characterized by a meridional dipole in the sea level pressure field, with centers of action near Iceland and the Azores. It has a profound influence on the weather, climate, ecosystems, and economies of Europe, Greenland, eastern North America, and North Africa. It has been proposed that around 1980, there was an eastward secular shift in the NAO's northern center of action that impacted sea ice export through Fram Strait. Independently, it has also been suggested that the location of its southern center of action is tied to the phase of the NAO. Both of these attributes of the NAO have been linked to anthropogenic climate change. Here the authors use both the one-point correlation map technique as well as empirical orthogonal function (EOF) analysis to show that the meridional dipole that is often seen in the sea level pressure field over the North Atlantic is not purely the result of the NAO (as traditionally defined) but rather arises through an interplay among the NAO and two other leading modes of variability in the North Atlantic region: the East Atlantic (EA) and the Scandinavian (SCA) patterns. This interplay has resulted in multidecadal mobility in the two centers of action of the meridional dipole since the late nineteenth century. In particular, an eastward movement of the dipole has occurred during the 1930s to 1950s as well as more recently. This mobility is not seen in the leading EOF of the sea level pressure field in the region.

## 1. Introduction

Teleconnections—long-range, spatially coherent, and time-varying regions of correlation or anticorrelation in the sea level pressure and other atmospheric fields—are extremely important manifestations of low-frequency climate variability (Wallace and Gutzler 1981, hereafter WG; Hurrell 1996). The North Atlantic Oscillation (NAO), a meridional ''seesaw'' or dipole in atmospheric pressure with centers of action near the Azores and Iceland, is among the most significant of these teleconnections (Van Loon and Rogers 1978; Hurrell 1995; Visbeck et al. 2001; Hurrell et al. 2003b). The NAO's centers of action correspond to the Icelandic low and the Azores high. Winters corresponding to the positive phase of the NAO are characterized by anomalously high (low) sea level pressure in the southern (northern) center of action. During this phase, temperatures tend to be colder in Greenland and North Africa but warmer in Scandinavia and in the southeastern United States (Hurrell et al. 2003b). A number of other phenomena have also been tied to the NAO, including shifts in the location of the North Atlantic storm track, precipitation over Europe and North Africa, the frequency of Greenland tip jets, sea ice transport through Fram Strait, deep ocean convection in the subpolar North Atlantic, and North Atlantic marine productivity (Dickson et al. 1996; Rogers 1997; Hilmer and Jung 2000; Hurrell et al. 2003a; Moore 2003; Våge et al. 2009; Hurrell and Deser 2009).

Although the NAO's centers of action have well-defined climatological locations, there exists considerable variability in their locations on a month-to-month

*Corresponding author address:* Dr. Kent Moore, University of Toronto Physics, 60 St. George Street, Toronto ON M5S 1A7, Canada. E-mail: gwk.moore@utoronto.ca

DOI: 10.1175/JCLI-D-12-00023.1

basis. For example, Mächel et al. (1998) used the Comprehensive Ocean–Atmosphere Data Set (COADS) sea level pressure data to show that the locations of the Icelandic low and Azores high during a particular month are usually delimited by the areas 40°–70°N, 55°–5°W and 20°–50°N, 55°–5°W. In addition, it has been shown that there is seasonal variability in the centers of action of the NAO, with the centers being located off the east coast of North America during the warm period of the year (Portis et al. 2001).

Around 1980 there was an eastward shift in the NAO's northern center of action which had an impact on sea ice export through Fram Strait (Hilmer and Jung 2000; Jung et al. 2003). It has also been independently suggested that there is mobility in the NAO's southern center of action related to its phase: it tends to be situated in the vicinity of the Azores when the NAO is in its negative phase and near the Iberian Peninsula during its positive phase (Cassou et al. 2004). This observed mobility has been hypothesized to be a consequence of anthropogenic climate change, which has, in some climate modeling studies, led to more frequent positive NAO states and thus an intrinsic eastward displacement (Ulbrich and Christoph 1999; Hu and Wu 2004). However, this effect is not present in all models, and, if present, it is generally small in magnitude (Stephenson et al. 2006). This is consistent with evidence of deficiencies in the ability of the current generation of climate models to simulate the NAO (Woollings et al. 2010b).

There is also evidence of longer-term variability in the centers of action of the NAO. In particular, Vicente-Serrano and Lopez-Moreno (2008) showed that there was nonstationarity in the relationship between the NAO and European precipitation that was associated with multidecadal variability in the locations of the NAO's centers of action. The climate record in the Greenland Ice Sheet Project (GISP2) ice core from Greenland exhibits a complex relationship with the NAO that has been proposed to be modulated by variability in the location of its northern center of action (Dawson et al. 2007). Along similar lines, a recent modeling study suggests that the transition between the Medieval Climate Anomaly and the Little Ice Age was also associated with a northeastward shift in the locations of the centers of action of the NAO (Trouet et al. 2009).

Empirical orthogonal function (EOF) analysis of the sea level pressure field over the North Atlantic region indicates that a meridional dipole with centers of action near Iceland and the Azores is the leading mode of variability (Barnston and Livezey 1987). It has been conventional in many studies to refer to this mode as *being synonymous* with the NAO, although more recently it has been pointed out that the NAO can by diagnosed via nonlinear techniques such as cluster analysis (Cassou et al. 2004; Hurrell and Deser 2009). As we shall discuss later, an EOF-based analysis in and of itself, does not capture the mobility that is associated with the meridional dipole in the regional sea level pressure field. As a consequence, we argue that it may be necessary to refine our teleconnection nomenclature with respect to the North Atlantic to differentiate between the canonical NAO, as captured in EOF analyses, and its actual manifestation as a meridional dipole in the sea level pressure field, as captured using other techniques.

The second and third leading EOFs of the North Atlantic region are structures with primary centers to the west of Ireland, in the case of the second leading mode, and near Bergen, Norway, in the case of the third leading mode (Barnston and Livezey 1987). These modes are commonly referred to as the East Atlantic (EA) and Scandinavian (SCA) patterns, respectively (although Barnston and Livezy called the latter the Eurasian pattern). Neither of these modes is as well studied as the NAO, but both play a role in the climate of the North Atlantic region. For example, the EA pattern modulates precipitation over southwest England and the Iberian Peninsula (Rodriguez-Puebla et al. 1998) and influences the position of the primary North Atlantic storm track and jet streams (Seierstad et al. 2007; Woollings et al. 2010a). Moore et al. (2011) showed that EA pattern played a role in anomalous NAO positive conditions that occurred during the winter of 2007, forcing more frequent barrier winds along the southeast coast of Greenland (Renfrew et al. 2008; Petersen et al. 2009). In addition, it has been proposed that the EA pattern, in conjunction with the NAO, was responsible for the extremely cold temperatures over Europe during December 2010 (Moore and Renfrew 2012). The SCA pattern has been shown to influence precipitation, temperatures, and cyclone activity across northern Europe and Eurasia (Bueh and Nakamura 2007; Seierstad et al. 2007).

In this paper, we investigate the extent to which a full characterization of the meridional dipole in sea level pressure over the North Atlantic, in particular the strength and location of its centers of action, requires knowledge not contained in a conventional NAO index. We show instead that it requires information embedded within the indices used to define the EA and SCA. This approach builds upon the work of Franzke and Feldstein (2005), as well as that of Moore et al. (2011) and Moore and Renfrew (2012). In particular, it assumes that the dipole characteristic of the sea level pressure field over the North Atlantic is not solely the result of what we refer to as the NAO, but rather is a continuum formed by the linear combination of the teleconnections that we

refer to as the NAO, the EA, and the SCA. The approach provides a simpler and arguably more heuristic alternative to nonlinear techniques such as cluster analysis or self-organizing maps (e.g., Cassou et al. 2004).

We accomplish this by revisiting one of the earliest studies to document the spatial structure of the NAO, which used the so-called one-point correlation map technique developed by WG. That study identified two locations, situated near Iceland and the Azores, where the magnitude of the spatial cross-correlation in the sea level pressure field was highest. WG described these as being the centers of action of the NAO. They focused their attention on a 15-yr-long period extending from December 1962 through February 1977. We show that the same analysis technique on a longer time period identifies multidecadal mobility in these centers of action that was not identified by WG or captured by an EOF analysis that identifies the NAO, EA, and SCA as the leading modes of variability in the North Atlantic region. Rather, it is only through the consideration of the magnitude and phases of these three teleconnections that it is possible to fully characterize the variability in the sea level dipole. Furthermore, using long-term indices of these three teleconnections, we present evidence of multidecadal mobility in each of their centers of action that extends back into the late nineteenth century.

## 2. Methods and data

Two main techniques, one-point correlation maps and empirical orthogonal function analysis, have been proposed to provide an objective characterization of the spatial structure of atmospheric teleconnections. Both have a common origin in the covariance matrix element $C_{iji'j'}$ for a latitude–longitude gridded atmospheric field $F_{ij}(t)$ defined as follows:

$$C_{iji'j'} = \langle F_{ij}, F_{i'j'} \rangle,$$

where $\langle A, B \rangle$ is the temporal covariance coefficient between $A(t)$ and $B(t)$.

The one-point correlation map technique calculates the teleconnectivity matrix $\mathbf{T}$ by determining for each grid point the minimum value of $\mathbf{C}$ (see WG). That is,

$$T_{ij} = |\min(C_{iji'j'})| \forall i'j'.$$

The conventional interpretation (WG) is that local maxima in $\mathbf{T}$ indicate centers of action of teleconnections. Furthermore, dipolar teleconnections such as the NAO have a symmetry between their two centers of action, $(i_n, j_n)$ and $(i_s, j_s)$, $T_{i_n j_n} = T_{i_s j_s}$.

A more complete description is provided by the EOF approach. With this technique one finds the eigenfunctions of the covariance matrix $C_{iji'j'}$ (Monahan et al. 2009). These eigenfunctions represent a set of spatial structures or basis functions that by definition explain the maximum amount of spatial variability in the underlying atmospheric field with the smallest number of spatial patterns (Monahan et al. 2009). A reconstruction of the field in question is then provided by

$$F_{ij}(t) = \sum_{k=1}^{N} \alpha_k e_{ij}^k,$$

where $e_{ij}^k$ is the $k$th eigenvector and $\alpha_k$ is the $k$th principal component (i.e., the projection of $F_{ij}$ onto $e_{ij}^k$).

Both techniques have their advantages and disadvantages. The one-point correlation map approach is only able to identify the leading correlation structure in a given region and, as a result, does not provide any information on the nonleading modes of variability. In addition, we will argue that the one-point correlation map technique does not capture the canonical leading teleconnection but rather the dominant correlation field that results from the *combined influences* of all the leading teleconnections in that region. By definition, the field identified with the one-point correlation map technique can be interpreted locally and does not depend on the shape of the domain used (Ambaum et al. 2001). On the other hand, EOFs are nonlocal in that their values at two different points depend on the entire covariance matrix (Monahan et al. 2009) As a result, points with the same sign in an EOF are not necessarily correlated (Ambaum et al. 2001). In addition, this nonlocal nature of the EOF analysis implies that the shape of the domain used impacts the spatial structure of the EOFs (Richman 1986).

In our application of the one-point correlation map technique and EOF analysis, we use the sea level pressure field from the National Centers for Environmental Research (NCEP) reanalysis for the 189 winter months [December–February (DJF)] from December 1948 to February 2011. The climatological monthly mean based on this entire period was used to calculate the anomalies from which the covariance matrix was calculated. For a longer-term perspective, we repeated the analysis using the sea level pressure field from the Twentieth-Century Reanalysis (20CR) Project (Compo et al. 2011). This reanalysis dataset assimilates only surface pressure observations and provides the first three-dimensional representation of the state of the troposphere in the

period prior to the establishment of the synoptic-scale upper-air network in the late 1940s (Compo et al. 2006, 2011). We use the 414 winter months (DJF) of the 20CR for its entire period from January 1871 to December 2008 with the climatological monthly mean again based on the entire period.

With respect to the one-point correlation technique, all other steps in the analysis procedure are the same as those used in WG. Indeed as shown in the appendix, we also calculated the sea level pressure teleconnectivity matrix **T** for the two periods used by WG using both the NCEP data (Kalnay et al. 1996; Kistler et al. 2001) and the 40-yr European Centre for Medium-Range Weather Forecasts (ECMWF) Re-Analysis (ERA-40; Uppala et al. 2005) and found excellent agreement with respect to the centers of action and the magnitude of the teleconnectivity matrix at these points.

With regard to the EOF analysis, we performed a latitude-weighting of the data prior to the calculation of the covariance matrix as recommended by Hannachi et al. (2007). The domain used for the EOF analysis covers the entire North Atlantic region and extends from 10° to 80°N and from 100°W to 40°E. No rotation of the eigenfunctions was applied. Although we computed the full spectrum of EOFs of the sea level pressure field, we focus our attention on the three leading EOFs that represent the NAO, EA, and SCA teleconnections. Indices of the NAO, EA, and SCA were calculated from the principal component time series of the three leading EOFs and, by construction, these indices are uncorrelated (Monahan et al. 2009).

## 3. Results

As discussed above, the teleconnectivity matrix **T** is essentially a measure of the point-wise cross-correlation in a given field. The calculation of **T** for the monthly mean sea level pressure field from the NCEP Reanalysis for the winter months (DJF), from 1948 to 2011, reveals two centers of action represented by broad regions of elevated correlations that are oriented in a southwest to northeast direction (Fig. 1). Embedded within each region are two localized maxima. For the northern center of action, one maximum is located between Cape Farewell (southern tip of Greenland) and southwest Iceland, while the other is located to the northeast of Iceland. For the southern center of action, the two maxima are located to the southwest of the Azores and over the Iberian Peninsula, respectively. As discussed in the appendix, examination of **T** for the primary period used by WG, winter of 1962/63 to the winter of 1976/77, shows only the western maximum for each of the two centers of action. For the other period used by WG, winter of 1949/50 to winter of 1961/62, again only the western maxima were identified. There was, however, a westward shift in their locations that was not commented upon by WG.

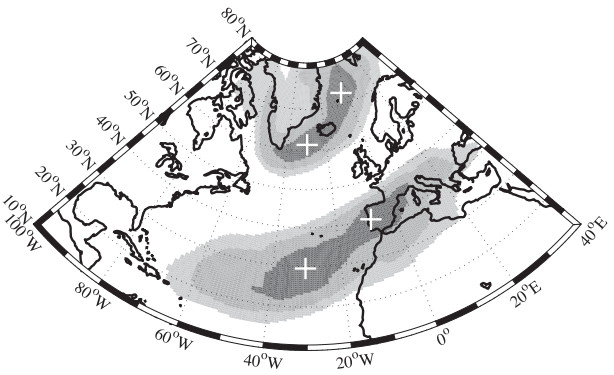


FIG. 1. Teleconnectivity matrix of the NCEP sea level pressure field for the winter months (DJF) from 1948 to 2011. The plus signs (+) indicate maxima in the teleconnectivity matrix. The lighter, medium, and darker shading represent teleconnectivity matrix values >0.6, 0.65, and 0.7, respectively.

Using the longer time series of the 20CR product, we computed the teleconnectivity matrix **T** for the monthly mean sea level pressure field for the winter months (DJF) from 1871 to 2008, as well as for two equal-length (180 month) subperiods from 1888 to 1948 and from 1948 to 2008 (Fig. 2). It should be noted the magnitude of the teleconnectivity matrix for the full period, 1871–2008, is smaller than that for the subperiods as a result of the longer time series used in its calculation. For all three periods, the teleconnectivity matrix retains the double maxima in each of the centers of action identified in Fig. 1. In particular, the presence of the double maxima during the earlier subperiod (Fig. 2b) is strongly suggestive that the eastward movement during the 1980s is not unique. It should be noted, however, that there is some variability in the position: in particular, during the later subperiod (Fig. 2c) the maxima in each center of action are more widely separated than during the earlier subperiod (Fig. 2b). In addition, the locations of the maxima during the later subperiod closely match those for the NCEP teleconnectivity matrix for the same period as well as the period 1948–2011 shown in Fig. 1.

Next we present the three leading EOFs calculated from the winter (DJF) monthly mean sea level pressure field from both the NCEP reanalysis and the 20CR (Fig. 3). The EOFs were calculated, in the case of the NCEP reanalysis, over the period from 1948 to 2011 and the three leading EOFs respectively describe 36%, 17.5%, and 15% of the variability in the sea level pressure field over this time period. The 20CR EOFs were

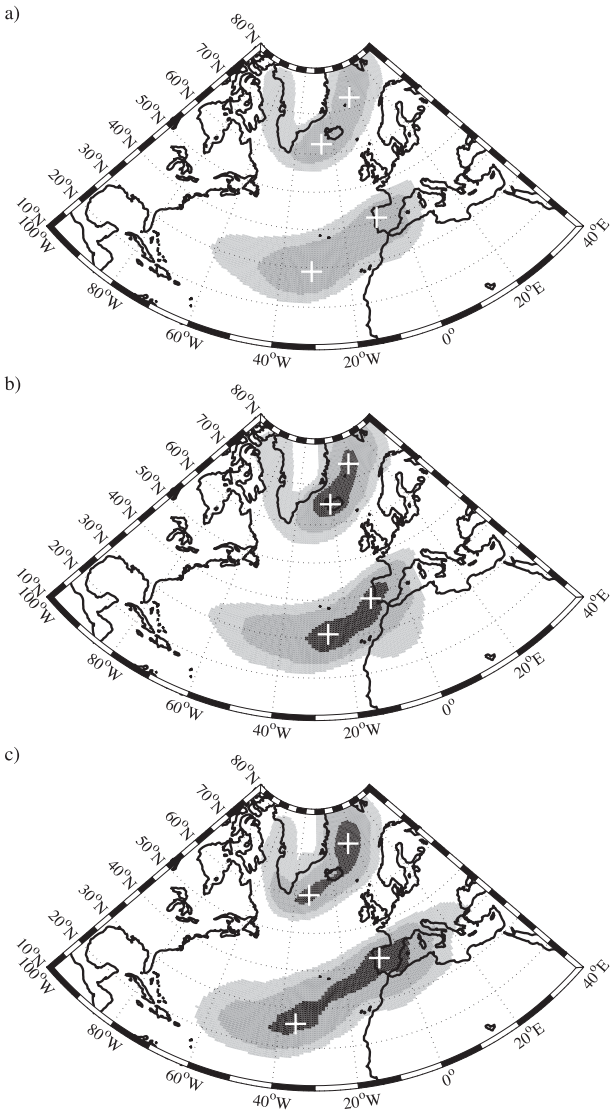


FIG. 2. As in Fig. 1, but for the 20CR sea level pressure field for the winter months (DJF) of (a) 1871–2008, (b) 1888–1948, and (c) 1948–2008.

calculated over the period 1871–2008 and the three leading EOFs respectively describe 33%, 20%, and 15% of the variability. The three leading EOFs represent the canonical NAO (Figs. 3a,b), EA (Figs. 3c,d), and SCA (Figs. 3e,f) teleconnections. Comparing the structure of the EOFs for the two periods and datasets indicates that there is good overall agreement as to the structure and magnitude. The NAO is characterized by a dipole structure with centers of action near Iceland and the Azores. The EA is a monopole structure with a center of action south of Iceland. Note that the center of action of the EA lies along the nodal line of the NAO (Moore and Renfrew 2012). The SCA is a monopole structure with a center of action situated in western Norway. There is evidence of a weak dipole associated with the SCA with a center of action of opposing sign situated over southern Greenland and the Labrador Sea.

EOFs are dependent on the chosen domain over which they are calculated (Ambaum et al. 2001; Monahan et al. 2009) and so one might wonder about the robustness of the features that we have presented in Fig. 3. As a check, we computed the spatial correlation fields of the winter (DJF) monthly mean sea level pressure field from the 20CR for the period 1871–2008 against indices of the NAO, EA, and SCA derived from the principal components of the corresponding EOF analysis. We show these fields in Fig. 4. For the most part, the spatial correlations are similar to the EOFs with respect to the location and structure of the respective centers of action. The EA and SCA spatial correlation fields exhibit side-lobe behavior that result in a tripole and quadrupole structures, respectively, that are also present, although in a more muted form, in the EOFs. Similar results were obtained with indices derived from the gridpoint sea level pressure at the respective centers of action, as did the corresponding analyses with the NCEP reanalysis.

Although the EOF analysis provides a bulk measure of the variability in the underlying field, it does not give information as to the spatial distribution of variability that is described. The spatial correlation technique allows for this and in Fig. 5 we show the percentage of the variability in the winter (DJF) monthly mean sea level pressure field from the 20CR for the period 1871–2008 that is described by the NAO, EA, and SCA. This was computed by summing the squares of the correlation coefficients shown in Fig. 4. A similar solution was obtained from the simultaneous multiple linear correlation coefficient analysis against indices of the NAO, EA, and SCA (Moore and Renfrew 2012). As one can see, the three modes describe over 50% of the variability over much of the North Atlantic, Greenland, northern Europe, and the eastern Canadian Arctic, with a maximum of over 90% in the vicinities of the centers of action of the EA and SCA.

Given the structure of the EOF patterns over the period 1871 to the present, it stands to reason that the NAO teleconnection, as described by the leading EOF of the sea level pressure field, in and of itself cannot be solely responsible for the occurrence of the multiple maxima in the teleconnectivity matrix identified in Figs. 1 and 2. In Fig. 6 we present linear combinations of the two leading EOFs [i.e., the NAO and EA for the 20CR winter (DJF) monthly mean sea level pressure field for the period 1871–2008]:

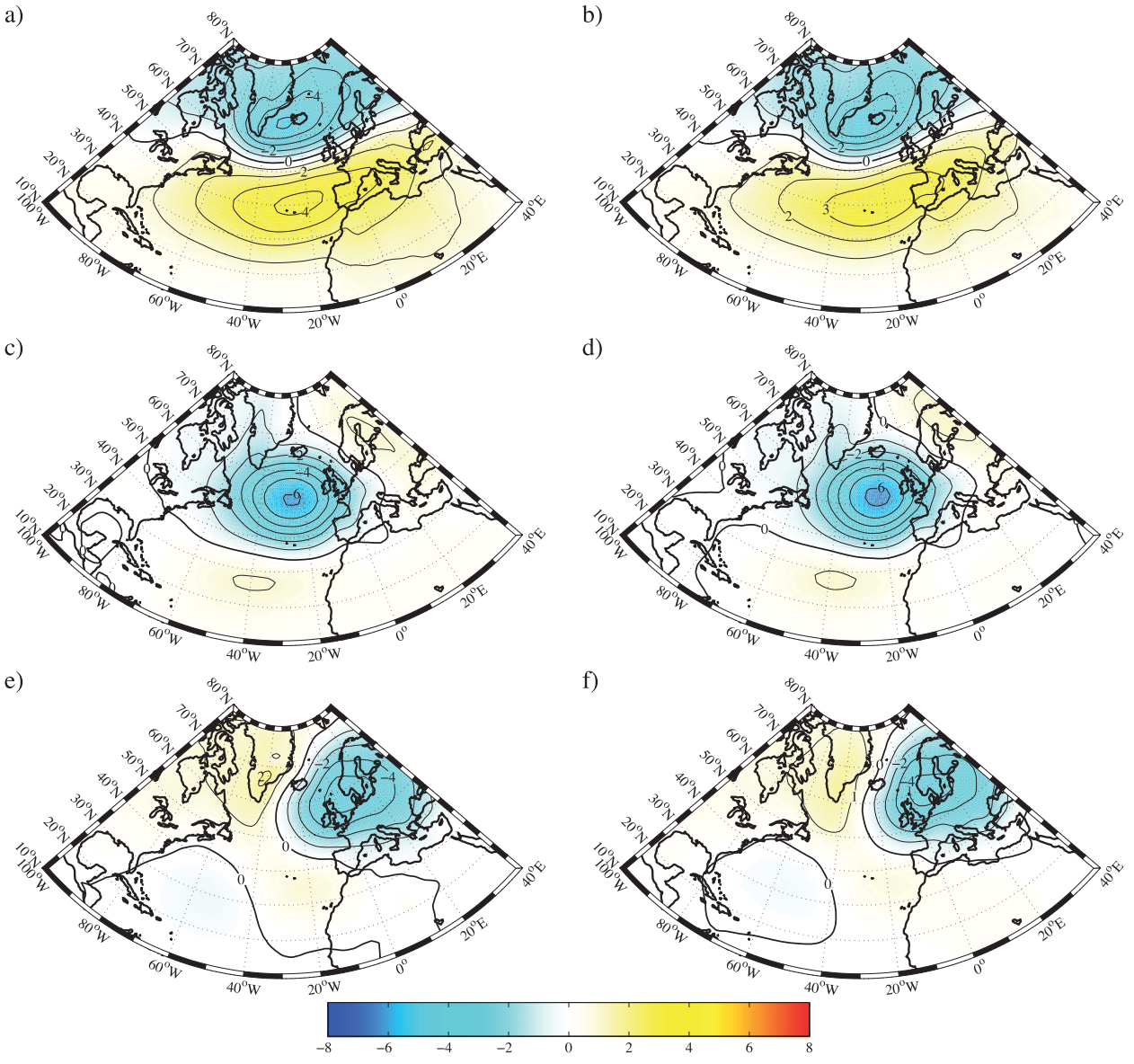


FIG. 3. The three leading EOFs of the sea level pressure field for the winter months (DJF). (left) The NCEP reanalysis for the period 1948–2011 and (right) the 20CR for the period 1871–2008. (a),(b) The leading EOF represents the NAO teleconnection, while the (c),(d) second and (e),(f) third represent the EA and SCA teleconnections, respectively.

$$\text{slp} = \alpha \times \text{NAO} + \beta \times \text{EA},$$
$$\text{where} \quad \alpha = \{-1, 0, 1\} \quad \text{and}$$
$$\beta = \{-1, 0, 1\}.$$

The cases where $\alpha = \pm 1$ and $\beta = 0$ represent the two phases of the NAO teleconnection, while the cases where $\alpha = 0$ and $\beta = \pm 1$ represent the two phases of the EA teleconnection. The remaining four cases where $\alpha = \pm 1$ and $\beta = \pm 1$ represent states associated with mixtures of the two teleconnections. Of course, other values of $\alpha$ and $\beta$ are possible; however, the combinations shown in Fig. 6 are sufficient to document the impact that the EA teleconnection has on the NAO. In all cases in which $\alpha \neq 0$, one can see that there exists a meridional dipole in the sea level pressure field. The cases where $\alpha$ and $\beta$ are of the same sign (e.g., $\alpha = 1$ and $\beta = 1$ or $\alpha = -1$ and $\beta = -1$) result in a southwestward movement in the centers of action of the dipole. On the other hand, the cases where they are of opposing sign result in a northeastward movement of the centers of action of the dipole. Thus, linear combinations of these EOFs result in southwest to northeast movement in the

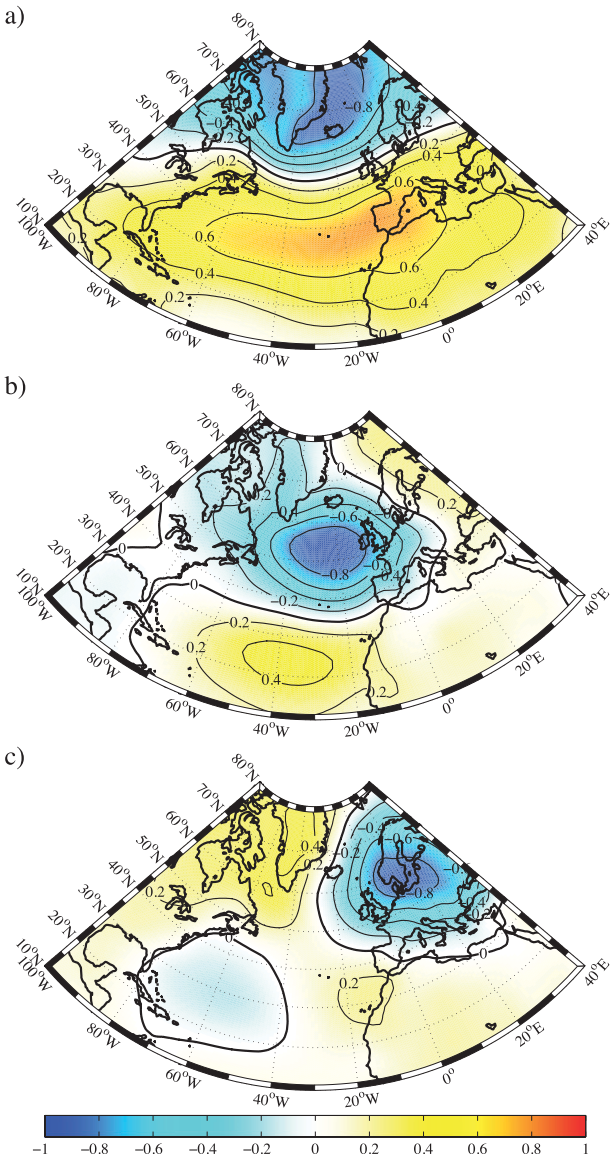


FIG. 4. Spatial correlation of the winter (DJF) monthly mean sea level pressure field from the 20CR for the period 1871–2008 against indices of the (a) NAO, (b) EA, and (c) SCA.

centers of action of the meridional dipole in sea level pressure.

The analogous linear combinations of the first and third leading EOFs (i.e., the NAO and SCA) are presented in Fig. 7:

$$\text{slp} = \delta \times \text{NAO} + \varepsilon \times \text{SCA},$$
$$\text{where} \quad \delta = \{-1, 0, 1\} \quad \text{and}$$
$$\varepsilon = \{-1, 0, 1\}.$$

The interpretation is similar to that for the linear combinations of the two leading EOFs. Again, one has, in all cases with $\delta$ nonzero, a meridional dipole in the sea level pressure field. The cases where $\delta$ and $\varepsilon$ are of the same sign result in a clockwise rotation in the centers of action (e.g., an eastward movement in the northern center of action and a westward movement in the southern center of action). The cases where they are of opposing sign result in a counterclockwise rotation in the centers of action.

It is of course possible to consider linear combinations of the three leading EOFs. However, given the results presented in Figs. 6 and 7 it clear that one must distinguish between the "pure" NAO teleconnection, which would exist only if the magnitude of the EA and SCA were zero, and the "NAO-like" meridional dipole in the sea level pressure field that exists when the magnitudes of the EA and SCA are nonzero. Furthermore, the results presented in Figs. 6 and 7 indicate that the binary interaction between the NAO and either the EA or the SCA can result in mobility in the centers of action of the meridional dipole in the sea level pressure field over the North Atlantic that was identified in the teleconnectivity matrix. This implies that the observed mobility in the two centers of action of the meridional dipole that occurred in the 1980s (Hilmer and Jung 2000; Cassou et al. 2004) can *potentially* be explained with reference to these other climate modes.

To confirm this, we use indices of the NAO (NAOI), EA (EAI), and SCA (SCAI) derived from the principal components of the EOF expansion of the 20CR (see section 2). We show these indices in Fig. 8, after the application of a low-pass filter with a cutoff of 21 years. The transition from NAO negative conditions during the 1960s to NAO positive conditions in the 1990s is apparent, as is the recent transition back to NAO negative conditions (Hurrell 1995; Moore and Renfrew 2012). The period from the late 1890s to the 1930s can be seen as a period when the NAO was positive that was preceded by a period when the NAO was negative. From the 1930s to the 1960s the NAO was again predominately negative. The EA and SCA also exhibit periodic transitions between their positive and negative states with the EA undergoing a very recent transition from negative to positive states with the opposite occurring for the SCA. In addition, since the 1940s the magnitude of the SCA has generally been larger than that for the EA.

We focus on four 21-yr-long subperiods from this record to highlight the efficacy of using indices of the NAOI, EAI, and SCAI to diagnose variability in the centers of action of the meridional dipole in sea level pressure over the North Atlantic. Specifically, we consider the winters during 1910–30, 1930–50, 1950–70, and 1970–90. These periods are highlighted in Fig. 8. The

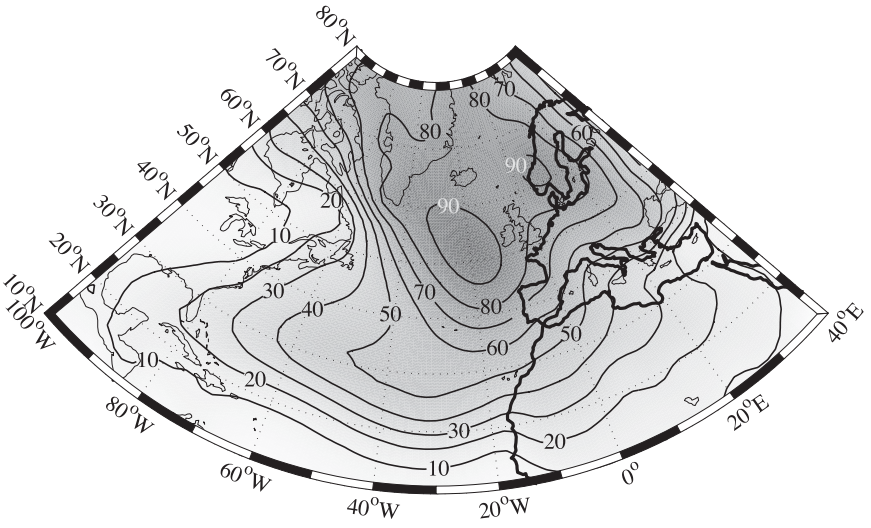


FIG. 5. Percentage of the variability in the winter (DJF) monthly mean sea level pressure field from the 20CR for the period 1871–2008 that is explained by the indices of the NAO, EA, and SCA.

teleconnectivity matrices from the sea level pressure field from the 20CR for these four periods are shown in Fig. 9. The first and third periods (Figs. 9a,c) have a single maximum in each center of action in the teleconnectivity matrix that is situated to the southwest of that associated with the pure NAO teleconnection (Figs. 3a,b). In contrast, the second and fourth periods (Figs. 9b,d) have maxima in the teleconnectivity matrix

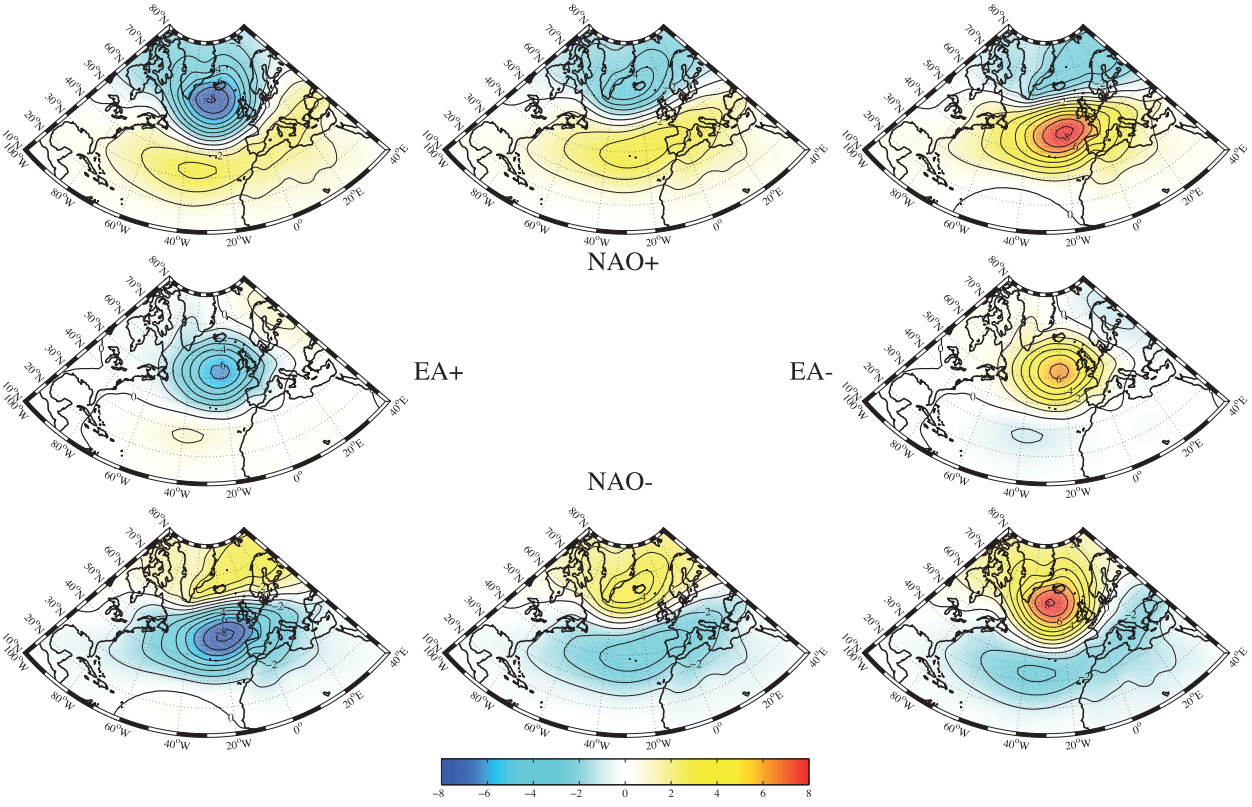


FIG. 6. Impact of the phase of the NAO and EA on the winter (DJF) monthly mean sea level pressure field (mb) over the North Atlantic. The figures in the middle column represent the leading EOF (i.e., the NAO), while those in the middle row represent the second leading EOF (i.e., the EA pattern). The corner figures represent the linear combinations of these two EOFS. The EOFs are from the 20CR for the period 1871–2008. Please refer to the text for more information on how the linear combinations were calculated.

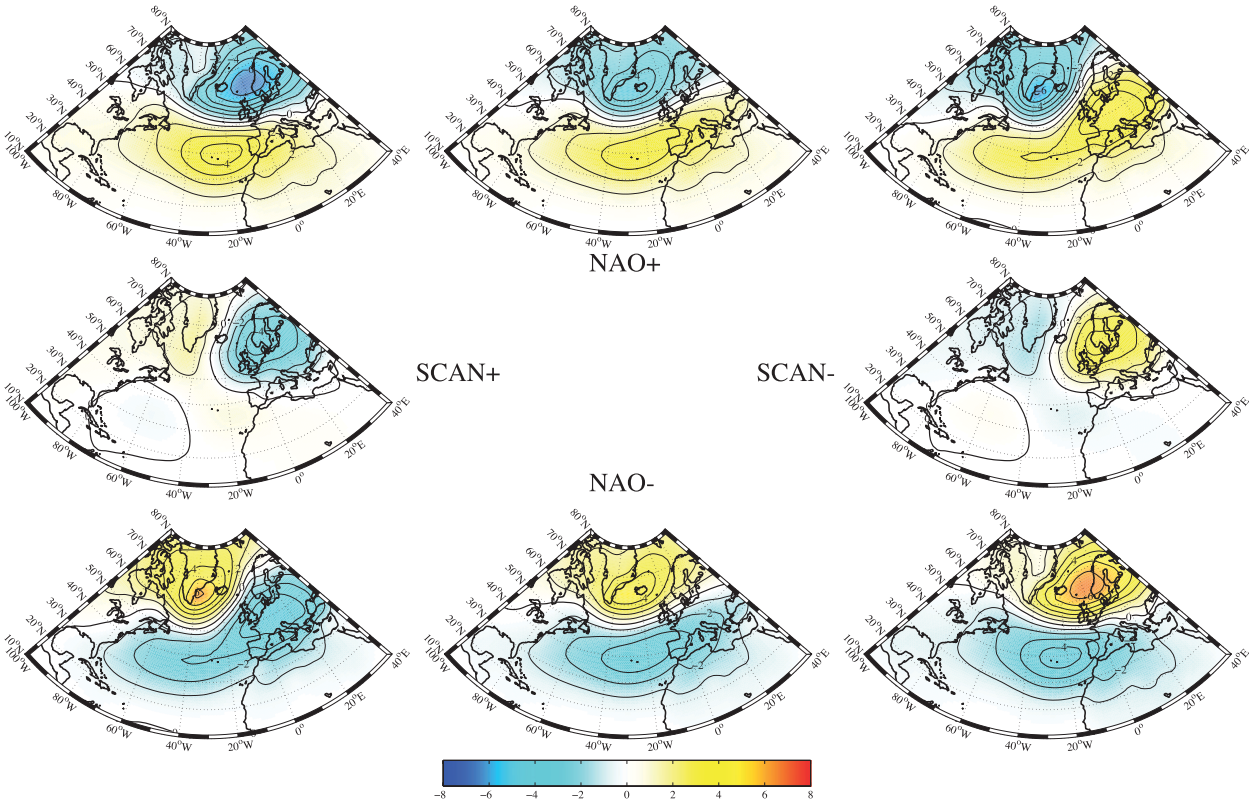


FIG. 7. As in Fig. 6, but for the SCA.

that are translated toward the northeast; in the case of the period 1930–50, there also exist (less extensive) secondary maxima to the southwest of the primary ones.

From Fig. 8, we note that during the first period (1910–30) the NAOI and EAI were both positive while the SCAI was predominately negative. The results from Figs. 3 and 4 imply a southwestward movement in the centers of action that is consistent with the teleconnectivity matrix of this period (Fig. 9a). During the second period (1930–50) the NAOI was for the most part negative while both the EAI and SCAI underwent changes in sign. In such a scenario, one would expect multiple centers of action as seen in the teleconnectivity matrix for this period (Fig. 9b). For the two latter periods, 1950–70 and 1970–90, the NAOI undergoes a change is sign with the EAI close to zero and the SCAI positive. From Fig. 4, one would thus expect the period 1950–70 to be one in which there was a southwestward shift in the centers of action, whereas the period 1970–90 should be one in which there was a northeastward shift. This is consistent with the teleconnectivity matrices for these two periods (Figs. 9c,d).

During the most recent period (i.e., after 1990), the NAO and the SCA were for the most part positive and the EA was negative. In this situation, one would again expect a northeastward shift in the centers of action, as is observed to be the case in the teleconnectivity matrix (not shown).

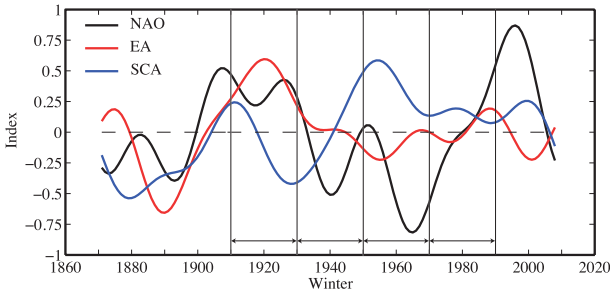


FIG. 8. Time series of the winter mean (DJF) indices of the NAO (black curve), EA (red curve), and SCA (blue curve) for the period 1871–2008. The indices are derived from the principal components of the EOF decomposition of the monthly mean winter (DJF) sea level pressure field from the 20CR. A low-pass filter with a cutoff of 21 years was used. The vertical lines delimit the periods investigated in further detail in Fig. 9.

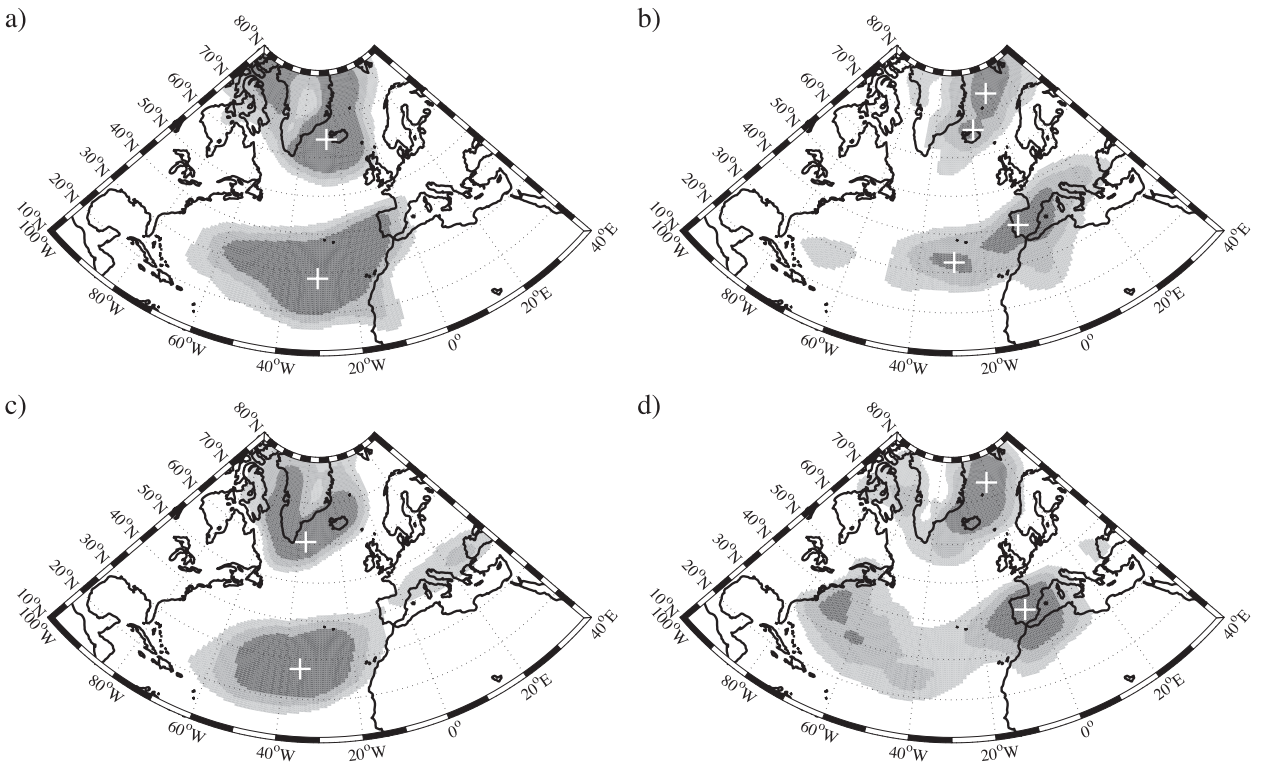


FIG. 9. Teleconnectivity matrix of the 20CR sea level pressure field for the winter months (DJF) of (a) 1910–30, (b) 1930–50, (c) 1950–70, and (d) 1970–90. The plus signs indicate maxima in the teleconnectivity matrix. The lighter, medium, and darker shading represent teleconnectivity matrix values >0.6, 0.65, and 0.7, respectively.

To confirm the stability of the structure of the leading EOF of the sea level pressure field over time, we show in Fig. 10 this EOF from the 20CR for the winters used in Fig. 9 (i.e., 1910–30, 1930–50, 1950–70, and 1970–90). The structure of this EOF is similar over the various subperiods and typically shows a well-defined dipole with centers of action near Iceland and the Azores. There are some minor differences in the orientation and location of the centers of action with the largest discrepancy occurring during the period from 1930 to 1950 when the southern center of action is shifted eastward. Although this a period where the teleconnectivity matrix shows an eastward shift in this center of action, the period from 1970 to 1990 during which the teleconnectivity matrix showed a similar shift is one in which the leading EOF shows no such shift. Figure 11 compares the structure of the leading EOF of the sea level pressure from the 20CR as calculated over the entire period 1871–2008 with the composite leading EOF calculated from all 21-yr-long windows during 1871–2008. Again the structure of the composite leading EOF is very similar to that calculated over the entire period, providing additional evidence as to the stability of its structure.

## 4. Summary and discussion

We have used the one-point correlation technique to revisit the analysis by WG with regard to North Atlantic teleconnection patterns in the sea level pressure field. By using longer datasets than those available to WG, we have shown that there exist multiple locations for the two centers of action associated with the NAO, with the dominance of one center of action over another changing with time. This behavior has been present since the late nineteenth century. However, it is not apparent in an EOF analysis of the sea level pressure field in the region, which indicates that the NAO has more or less fixed centers of action located near Iceland and the Azores.

As we illustrate in this paper, a full description of the meridional dipole in the sea level pressure field that we conventionally refer to as the NAO requires knowledge of two other teleconnections in the region that are commonly referred to as the East Atlantic (EA) and Scandinavian (SCA) patterns. These teleconnections are, after the NAO, the second and third leading teleconnections in the region. They each explain approximately 15%–20% of the variability in the winter sea

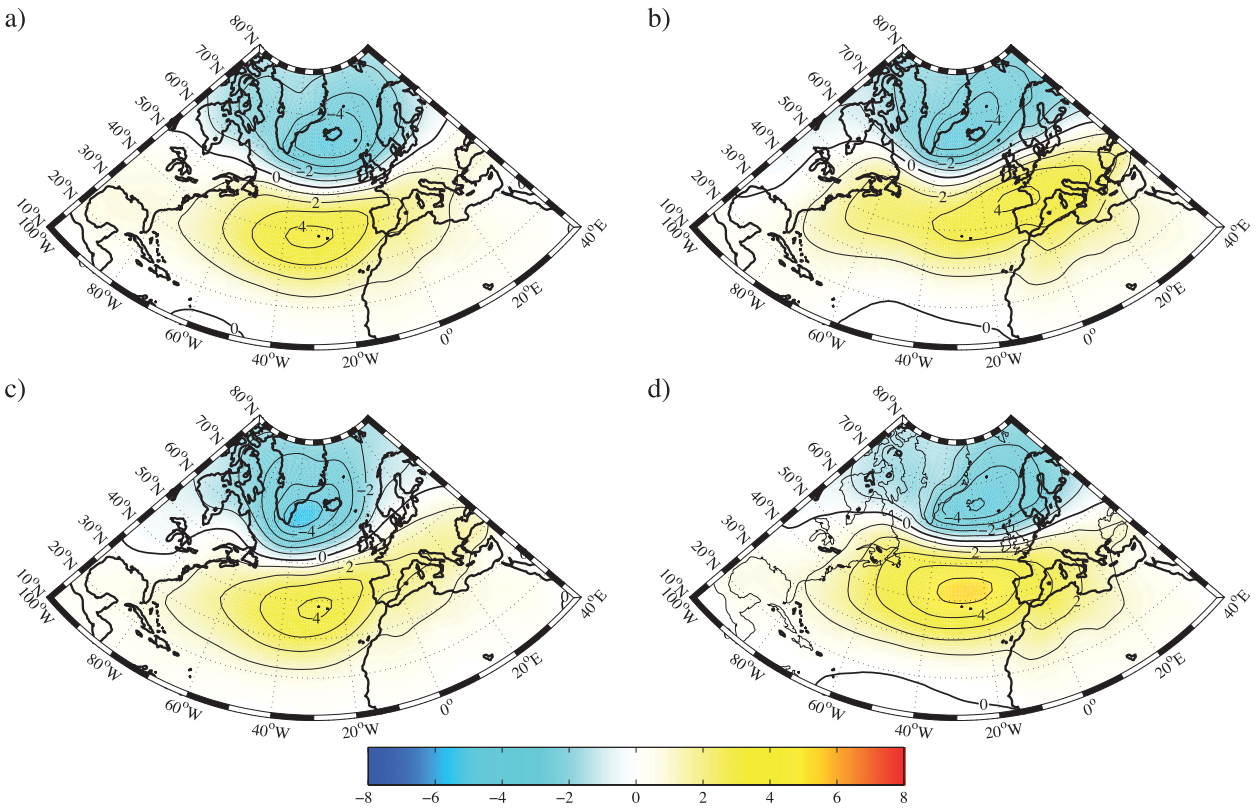


FIG. 10. The leading EOF of the sea level pressure field for the winter months (DJF) from the 20CR during (a) 1910–30, (b) 1930–50, (c) 1950–70, and (d) 1970–90.

level pressure field and so are not inconsequential when compared to the approximate 35% of the variability that is explained by the NAO. Indeed, recent studies have shown that they play an important role in the climate of the region (Seierstad et al. 2007; Woollings 2010; Woollings et al. 2010a; Moore et al. 2011; Moore and Renfrew 2012). Variability in the structure of the meridional dipole not captured by consideration of the NAO in isolation may help explain climate variability in the North Atlantic–western European–Greenland region that is uncorrelated or only weakly correlated with the NAO (Dawson et al. 2002, 2007; Vicente-Serrano and Lopez-Moreno 2008; Trouet et al. 2009; Holmes et al. 2010).

Linear combinations of the NAO and either the EA or SCA still result in a meridional dipole in the sea level pressure field over the North Atlantic but with centers of action that are displaced with respect to those associated with the ''pure'' NAO. When the phase of the NAO and EA are of the same sign, the centers of action are shifted to the southwest; when the phases are opposite, there is a shift to the northeast. When the phase of the NAO and SCA are of the same sign, there is a counterclockwise rotation in the centers of action, whereas when the phases are opposite there is a clockwise rotation.

Our results are novel in several regards. Firstly, they show that this mobility occurs simultaneously in both centers of action and not, as has been suggested previously, in either the northern (Hilmer and Jung 2000; Jung et al. 2003) or southern center of action only (Cassou et al. 2004). Secondly, they suggest that this mobility is not just a secular trend of the late twentieth century, as has been previously proposed (Hilmer and Jung 2000; Jung et al. 2003), but has occurred in the past as well. In particular, we have identified the period 1930–50 as one, similar to the period after the 1980s, in which the centers of action of the NAO were displaced toward the northeast. Between these times (1950–70) the centers of action were displaced toward the southwest. It was for this period that WG performed their analysis; as a result, they did not identify the multiple centers of action of the meridional dipole.

We have also shown that, in addition to the NAO, the EA and SCA both exhibit variability on multidecadal time scales. Our analysis suggests that it is important to consider this variability and its impact on the structure of the meridional dipole in sea level pressure in

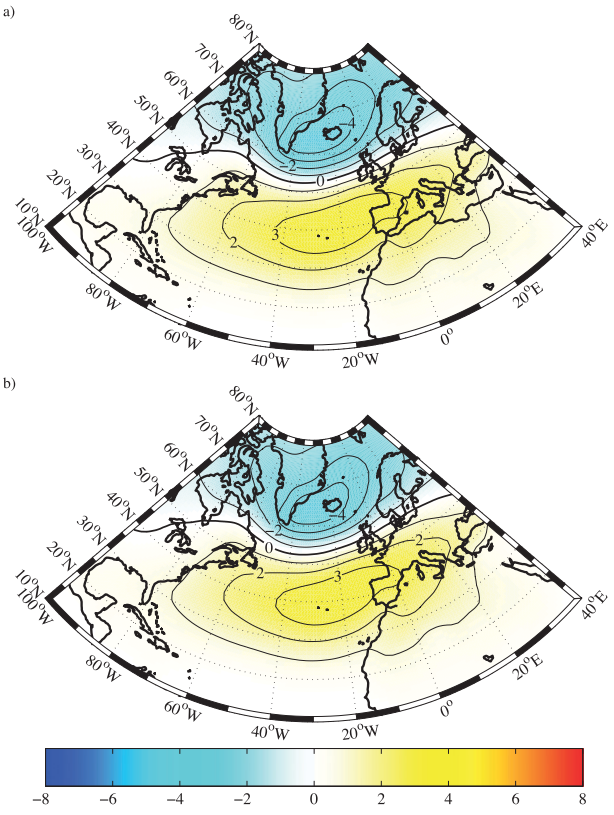


FIG. 11. (a) The leading EOF of the sea level pressure field for the winter months (DJF) from the 20CR for the period 1871–2008. (b) The composite of leading EOF of the sea level pressure field for the winter months (DJF) from the 20CR for all the 21-yr-long moving windows that cover the period 1871–2008.

diagnosing the climate signal associated with the NAO. This suggests that the NAO's mobility is an inherent part of the coupled climate system of the North Atlantic that, while affected by its phase (and thus anthropogenic climate change), has other governing factors as well.

Finally, our work suggests a reinterpretation of the teleconnectivity matrix and the one-point correlation map technique. As we have shown, it does provide information on the spatial structure of teleconnections that is fundamentally different from that provided by EOF analyses. In particular, it sheds light on the observed spatial correlations that are active in a given region over a given period of time. This is information that is not the result of a single (usually the leading) EOF, but rather is information that is the result of the continuum of EOFs that are active at that time (Franzke and Feldstein 2005). The fact that this technique can capture such fundamental characteristics of observed teleconnections as the mobility of their centers of actions suggests that its use in other applications may be warranted.

*Acknowledgments.* GWKM was supported by the Natural Sciences and Engineering Research Council of Canada. IAR was supported in part by NE/C003365/1. RSP was supported by Grant OCE-0959381 from the U.S. National Science Foundation. The NCEP Reanalysis and 20CR data were provided by the NOAA Climate Diagnostics Center.

## APPENDIX

### Comparison with the Wallace and Gutzler (1981) Analysis

The original WG study used fields from the National Weather Service's operational analysis for the 45 winter months (DJF) from December 1962 to February 1977, and as a test, their analysis was repeated with an independent sample of the 39 winter months (DJF) from December 1949 to February 1962 (WG). In each case, the climatological monthly means were subtracted from the fields and the covariance matrix was calculated using the resulting anomalies.

Figure A1 shows the NCEP reanalysis and ERA-40 sea level teleconnectivity matrix **T** for the period from December 1962 to February 1977. The color scale used is the same as in the original study (WG). Also shown are the maxima in **T** as well as arrows connecting grid points that have the largest anticorrelation on their respective one-point correlation maps. Comparison of Fig. A1 with the original figure from WG shows very good agreement with respect to the centers of action and the magnitude of the teleconnectivity matrix at these points.

Figure A2 shows the NCEP reanalysis sea level teleconnectivity matrix **T** for the period from December 1949 to February 1962. With regard to the North Atlantic, there again exists a single maximum associated with each center of action of the NAO. However, the locations of the maxima are shifted westward by approximately 20°. Although it was not commented up at the time, such a shift is also present in the original figure (WG).

Over the North Pacific, there are also significant changes between the two periods. In particular, the period from December 1962 to February 1977 was characterized by two separate dipolar patterns (Figs. A1 and A2) that were originally attributed to the North Pacific Oscillation and the Pacific–North American pattern (WG). The easternmost of these patterns is absent during the period from December 1949 to February 1962 and the westernmost pattern is shifted eastward by approximately 40°. These differences were attributed at the time to the fact that the time period used

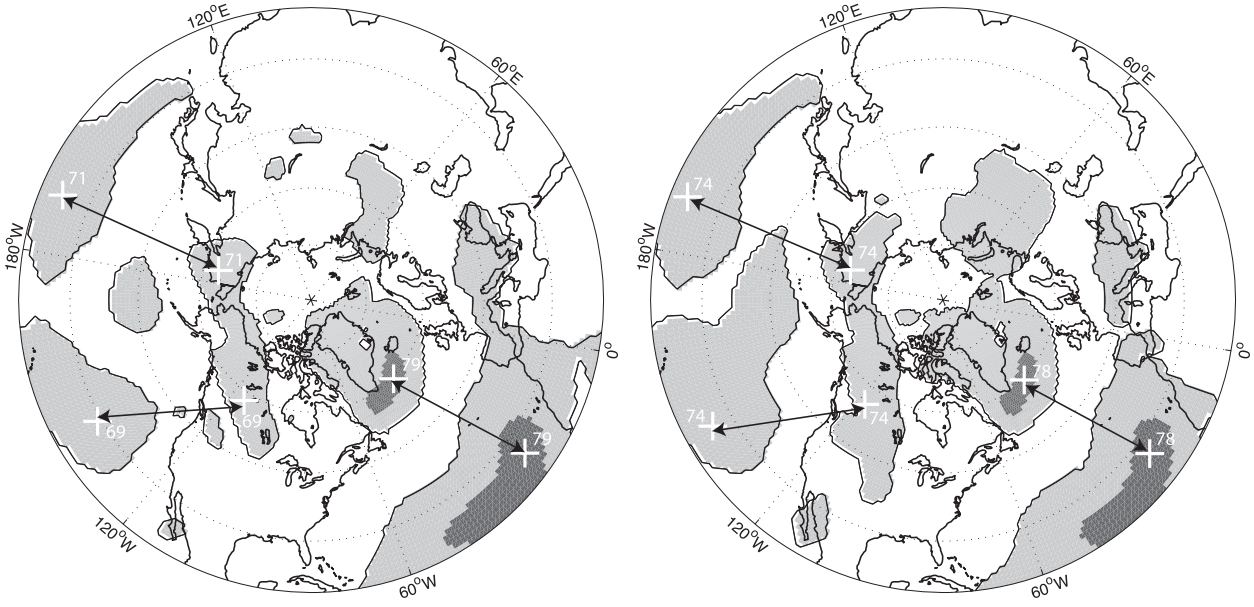


FIG. A1. Teleconnectivity matrix of the sea level pressure field for the winter months (DJF) from 1962/63 to 1977/78 as calculated from the (left) NCEP and (right) ERA-40 reanalyses. The centers of action are indicated as are the magnitudes. The shading matches that used by WG.

was too short to capture the variability in the system (WG). Given the results we have presented, it may be that the Pacific–North American pattern has a degree of variability with respect to the location of its centers of action as well.

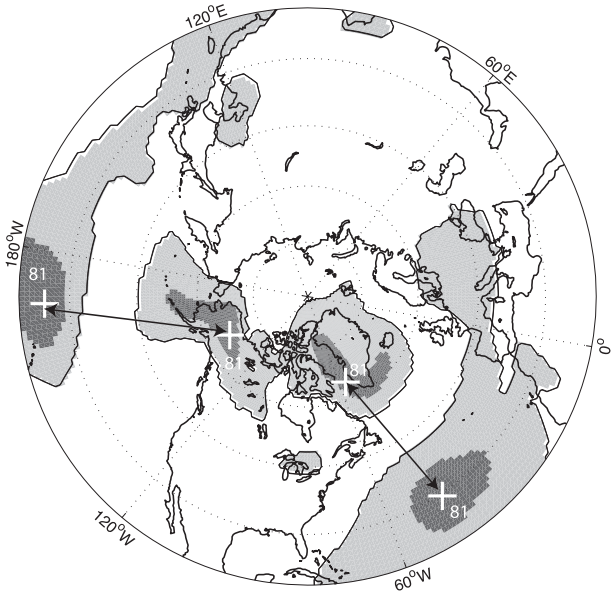


FIG. A2. Teleconnectivity matrix of the sea level pressure field for the winter months (DJF) from 1949/50 to 1961/62 as calculated from the NCEP reanalysis. The centers of action are indicated as are the magnitudes. The shading matches that used by WG.

## REFERENCES

Ambaum, M. H. P., B. J. Hoskins, and D. B. Stephenson, 2001: Arctic Oscillation or North Atlantic Oscillation? *J. Climate,* **14,** 3495–3507.

Barnston, A. G., and R. E. Livezey, 1987: Classification, seasonality, and persistence of low-frequency atmospheric circulation patterns. *Mon. Wea. Rev.,* **115,** 1083–1126.

Bueh, C., and H. Nakamura, 2007: Scandinavian pattern and its climatic impact. *Quart. J. Roy. Meteor. Soc.,* **133,** 2117–2131.

Cassou, C., L. Terray, J. W. Hurrell, and C. Deser, 2004: North Atlantic winter climate regimes: Spatial asymmetry, stationarity with time, and oceanic forcing. *J. Climate,* **17,** 1055–1068.

Compo, G. P., J. S. Whitaker, and P. D. Sardeshmukh, 2006: Feasibility of a 100-year reanalysis using only surface pressure data. *Bull. Amer. Meteor. Soc.,* **87,** 175–190.

——, and Coauthors, 2011: The Twentieth Century Reanalysis Project. *Quart. J. Roy. Meteor. Soc.,* **137,** 1–28.

Dawson, A. G., and Coauthors, 2002: Complex North Atlantic Oscillation (NAO) Index signal of historic North Atlantic storm-track changes. *Holocene,* **12,** 363–369.

——, K. Hickey, P. A. Mayewski, and A. Nesje, 2007: Greenland (GISP2) ice core and historical indicators of complex North Atlantic climate changes during the fourteenth century. *Holocene,* **17,** 427–434.

Dickson, R., J. Lazier, J. Meincke, P. Rhines, and J. Swift, 1996: Long-term coordinated changes in the convective activity of the North Atlantic. *Prog. Oceanogr.,* **38,** 241–295.

Franzke, C., and S. B. Feldstein, 2005: The continuum and dynamics of Northern Hemisphere teleconnection patterns. *J. Atmos. Sci.,* **62,** 3250–3267.

Hannachi, A., I. T. Jolliffe, and D. B. Stephenson, 2007: Empirical orthogonal functions and related techniques in atmospheric science: A review. *Int. J. Climatol.,* **27,** 1119–1152.

Hilmer, M., and T. Jung, 2000: Evidence for a recent change in the link between the North Atlantic Oscillation and Arctic sea ice export. *Geophys. Res. Lett.,* **27,** 989–992.

Holmes, J., and Coauthors, 2010: Climate and atmospheric circulation changes over the past 1000 years reconstructed from oxygen isotopes in lake-sediment carbonate from Ireland. *Holocene,* **20,** 1105–1111.

Hu, Z.-Z., and Z. Wu, 2004: The intensification and shift of the annual North Atlantic Oscillation in a global warming scenario simulation. *Tellus,* **56A,** 112–124.

Hurrell, J. W., 1995: Decadal trends in the North Atlantic Oscillation—Regional temperatures and precipitation. *Science,* **269,** 676–679.

——, 1996: Influence of variations in extratropical wintertime teleconnections on Northern Hemisphere temperature. *Geophys. Res. Lett.,* **23,** 665–668.

——, and C. Deser, 2009: North Atlantic climate variability: The role of the North Atlantic Oscillation. *J. Mar. Syst.,* **78,** 28–41.

——, Y. Kushner, G. Ottersen, and M. Visbeck, 2003a: An overview of the North Atlantic Oscillation. *The North Atlantic Oscillation: Climatic Significance and Environmental Impact, Geophys. Monogr.,* Vol. 134, Amer. Geophys. Union, 1–35.

——, ——, ——, and ——, Eds., 2003b: *The North Atlantic Oscillation: Climatic Significance and Environmental Impact. Geophys. Monogr.,* Vol. 134, Amer. Geophys. Union, 279 pp.

Jung, T., M. Hilmer, E. Ruprecht, S. Kleppek, S. K. Gulev, and O. Zolina, 2003: Characteristics of the recent eastward shift of interannual NAO variability. *J. Climate,* **16,** 3371–3382.

Kalnay, E., and Coauthors, 1996: The NCEP/NCAR 40-Year Reanalysis Project. *Bull. Amer. Meteor. Soc.,* **77,** 437–471.

Kistler, R., and Coauthors, 2001: The NCEP–NCAR 50-Year Reanalysis: Monthly means CD-ROM and documentation. *Bull. Amer. Meteor. Soc.,* **82,** 247–267.

Mächel, H., A. Kapala, and H. Flohn, 1998: Behaviour of the centres of action above the Atlantic since 1881. Part I: Characteristics of seasonal and interannual variability. *Int. J. Climatol.,* **18,** 1–22.

Monahan, A. H., J. C. Fyfe, M. H. P. Ambaum, D. B. Stephenson, and G. R. North, 2009: Empirical orthogonal functions: The medium is the message. *J. Climate,* **22,** 6501–6514.

Moore, G. W. K., 2003: Gale force winds over the Irminger Sea to the east of Cape Farewell, Greenland. *Geophys. Res. Lett.,* **30,** 1894, doi:10.1029/2003GL018012.

——, and I. Renfrew, 2012: Cold European winters: Interplay between the NAO and the East Atlantic mode. *Atmos. Sci. Lett.,* **13,** 1–8.

——, R. S. Pickart, and I. A. Renfrew, 2011: Complexities in the climate of the subpolar North Atlantic: A case study from the winter of 2007. *Quart. J. Roy. Meteor. Soc.,* **137,** 757–767.

Petersen, G. N., I. A. Renfrew, and G. W. K. Moore, 2009: An overview of barrier winds off southeastern Greenland during the Greenland Flow Distortion experiment. *Quart. J. Roy. Meteor. Soc.,* **135,** 1950–1967.

Portis, D. H., J. E. Walsh, M. El Hamly, and P. J. Lamb, 2001: Seasonality of the North Atlantic oscillation. *J. Climate,* **14,** 2069–2078.

Renfrew, I. A., and Coauthors, 2008: The Greenland flow distortion experiment. *Bull. Amer. Meteor. Soc.,* **89,** 1307–1324.

Richman, M. B., 1986: Rotation of principal components. *J. Climatol.,* **6,** 293–335.

Rodriguez-Puebla, C., A. H. Encinas, S. Nieto, and J. Garmendia, 1998: Spatial and temporal patterns of annual precipitation variability over the Iberian Peninsula. *Int. J. Climatol.,* **18,** 299–316.

Rogers, J. C., 1997: North Atlantic storm track variability and its association to the North Atlantic Oscillation and climate variability of northern Europe. *J. Climate,* **10,** 1635–1647.

Seierstad, I. A., D. B. Stephenson, and N. G. Kvamsto, 2007: How useful are teleconnection patterns for explaining variability in extratropical storminess? *Tellus,* **59A,** 170–181.

Stephenson, D. B., and Coauthors, 2006: North Atlantic Oscillation response to transient greenhouse gas forcing and the impact on European winter climate: A CMIP2 multi-model assessment. *Climate Dyn.,* **27,** 401–420.

Trouet, V., J. Esper, N. E. Graham, A. Baker, J. D. Scourse, and D. C. Frank, 2009: Persistent positive North Atlantic oscillation mode dominated the medieval climate anomaly. *Science,* **324,** 78–80.

Ulbrich, U., and M. Christoph, 1999: A shift of the NAO and increasing storm track activity over Europe due to anthropogenic greenhouse gas forcing. *Climate Dyn.,* **15,** 551–559.

Uppala, S. M., and Coauthors, 2005: The ERA-40 Re-Analysis. *Quart. J. Roy. Meteor. Soc.,* **131,** 2961–3012.

Våge, K., and Coauthors, 2009: Surprising return of deep convection to the subpolar North Atlantic Ocean in winter 2007–2008. *Nat. Geosci.,* **2,** 67–72.

Van Loon, H., and J. C. Rogers, 1978: Seesaw in winter temperatures between Greenland and northern Europe. 1. General description. *Mon. Wea. Rev.,* **106,** 296–310.

Vicente-Serrano, S. M., and J. I. Lopez-Moreno, 2008: Nonstationary influence of the North Atlantic Oscillation on European precipitation. *J. Geophys. Res.,* **113,** D20120, doi:10.1029/2008JD010382.

Visbeck, M. H., J. W. Hurrell, L. Polvani, and H. M. Cullen, 2001: The North Atlantic Oscillation: Past, present, and future. *Proc. Natl. Acad. Sci. USA,* **98,** 12 876–12 877.

Wallace, J. M., and D. S. Gutzler, 1981: Teleconnections in the geopotential height field during the Northern Hemisphere winter. *Mon. Wea. Rev.,* **109,** 784–812.

Woollings, T., 2010: Dynamical influences on European climate: An uncertain future. *Philos. Trans. Roy. Soc.,* **368A,** 3733–3756.

——, A. Hannachi, and B. Hoskins, 2010a: Variability of the North Atlantic eddy-driven jet stream. *Quart. J. Roy. Meteor. Soc.,* **136,** 856–868.

——, ——, ——, and A. Turner, 2010b: A regime view of the North Atlantic Oscillation and its response to anthropogenic forcing. *J. Climate,* **23,** 1291–1307.